Histochem Cell Biol (2008) 130:127–140
DOI 10.1007/s00418-008-0410-2

ORIGINAL PAPER

Epithelial and endothelial barriers in the olfactory region of the nasal cavity of the rat

Hartwig Wolburg · Karen Wolburg-Buchholz · Heike Sam · Sándor Horvát · Maria A. Deli · Andreas F. Mack

Accepted: 29 February 2008 / Published online: 14 March 2008

Abstract The olfactory ensheathing (glial) cells (OECs) have been identified to be useful candidate cells to support regeneration after being transplanted into injured fiber tracts of the central nervous system. We investigated by means of immunocytochemistry and freeze-fracturing the morphology and molecular composition of OEC tight junctions in the rat olfactory system. In addition, we tested the hypothesis whether tight junctions and orthogonal arrays of particles (OAPs) which contain the water channel protein aquaporin-4 (AQP4), are mutually exclusive as suggested in previous studies. In OECs, we found neither OAPs nor AQP4, but tight junctions immunoreactive for ZO-1, occludin, and claudin-5, but immunonegative for ZO-2 and claudin-3. To shed more light on the function of OEC tight junctions, we tested the permeability and tight junction composition of blood vessels and fila olfactoria. We found them both, permeable for infused lanthanum nitrate, and to be immunopositive for ZO-1 and claudin-5. The tight junctions of the OECs are discussed to be responsible for micro-compartmentalization within the olfactory fiber tract providing a benefit for axonal growth.

Keywords Olfactory system · Olfactory ensheathing cells · Aquaporins · Tight junctions · Freeze-fracturing

H. Wolburg (✉) · K. Wolburg-Buchholz · H. Sam
Institute of Pathology, University of Tübingen,
Liebermeisterstraße 8, 72076 Tübingen, Germany
e-mail: hartwig.wolburg@med.uni-tuebingen.de

S. Horvát · M. A. Deli
Institute of Biophysics, Biological Research Center,
6726 Szeged, Hungary

A. F. Mack
Institute of Anatomy, University of Tübingen,
72076 Tübingen, Germany

Introduction

Two salient features render the olfactory system an exciting area of research. First, the sensory neurons are embedded in an epithelium directly facing the external environment, the olfactory texture of which is relayed to the brain-giving rise to manifold behavioural reactions. Second, this cellular system is continuously renewing raising questions about the mechanism of continuous axonal growth and synaptic reorganization within the olfactory bulb (Graziadei and Monti Graziadei 1985; Mackay-Sim and Kittel 1991). The unmyelinated axons grow from the sensory neurons leaving the sensory epithelium as bundles termed fila olfactoria. All fila olfactoria together form the olfactory nerve traversing the cribriform plate and entering the olfactory bulb (see, for example, Li et al. 2005). The fila olfactoria are wrapped in glial cells and surrounded by perineural cells. The perineural cell sheath is continuous with the meningeal sheath where the olfactory fila enter the olfactory bulb. The glial cells embracing the axon bundles were identified in earlier studies as either astrocytes or Schwann cells, now generally known as olfactory ensheathing cells (OECs; Ramón-Cueto and Avila 1998). Some studies have addressed the molecular relationship of OECs to Schwann cells (Wewetzer et al. 2002; Bock et al. 2007) concluding that all OECs are Schwann cells which develop their characteristic phenotype under the specific influence of the olfactory system. Alternatively, the OECs and the Schwann cells can be viewed as unrelated due to their distinct embryonic origin, the olfactory placode and the neural crest, respectively (Jessen and Mirsky 2005). In any case, the two cell types display the following morphological difference: unmyelinating Schwann cells incorporate individual axons separating them from each other by their cytoplasm; OECs surround large groups of axons by extended processes allowing individual axons

to contact each other. In this aspect, OECs resemble astrocytes that also form extended processes embracing groups of neuronal processes. Schwann cells and OECs form a basal lamina at the interface to the interstitial space, astrocytes as well form a basal lamina where the CNS encounters mesenchymal spaces such as at the surface of the brain (superficial astroglial limiting membrane) or the blood vessels (perivascular astroglial limiting membrane).

The superficial and the perivascular astroglial endfeet membranes contain the orthogonal arrays of particles (OAPs) known from many freeze-fracture investigations since 1973 (Dermietzel 1973; for a comprehensive overview of the freeze-fracture literature, see Wolburg 1995). The OAPs are known today to contain the water channel protein aquaporin-4 (AQP4; Rash et al. 2004).

In an earlier freeze-fracture study, we showed that OECs were devoid of OAPs (Mack and Wolburg 1986). This result is now indirectly confirmed by the absence of AQP4 in OECs. The second result of our earlier study was the presence of tight junctions between OECs. In further investigations, we postulated a mutual exclusiveness of OAPs and tight junctions, at least in the CNS (Mack et al. 1987) and founded a concept according to that tight junction-connected glial cells might support axonal regeneration and/or growth (Wolburg et al. 1986). The phenomenological correspondence of presence of tight junctions, absence of OAPs and the steady growth of olfactory axons (or optic axons in fish) argued in favour of a functional relationship between these parameters. More recently, we have started to re-investigate this relationship by the observation of claudin-1-based, tight junction-related immunoreactivity in astrocytes surrounding bundles of newly formed axons within the fish optic nerve (Mack and Wolburg 2006).

The mutual exclusiveness of OAPs and tight junctions as mentioned above is also realized when comparing OECs and astrocytes. Mammalian astrocytes form OAPs but not tight junctions, mammalian OECs form tight junctions but not OAPs. Could this phenotype be related to the ability of continuous growth? In recent years, OECs have become a preferred cell population to be used in support for regeneration after CNS lesions (Li et al. 1997, 2005; Imaizumi et al. 2000; Raisman 2001; Barnett and Chang 2004; López-Vales et al. 2007). No study, however, has so far investigated tight junctions in the transplantation experiments using OECs in spinal cord lesions (Li et al. 1997).

In the present study, we have described the distribution of some antigens such as water channel proteins und tight junction proteins in different cells of the olfactory system of the rat by conventional and freeze-fracture electron microscopy as well as by confocal laser scanning immunocytochemistry. In addition, we performed experiments testing the permeability of blood vessels using the lanthanum nitrate method. Our motivation for this study was to shed light on the hypothesis that glia-related and tight junction-based compartmentalization of a nerve fibre tract as well as the modulation of the vascular permeability could be able to improve regeneration and growth conditions.

Materials and methods

Animals

Male Wistar rats (n = 5/groups; 315 ± 24 g, 3-month old) were used for this study. The experiments performed conform to European Communities ‘‘Council directive for the care and use of laboratory animals’’ and were approved by local authorities (XVI./03835/001/2006). The rats were anesthetized i.p. with Avertin solution (1.25%, 0.3 ml/kg b.w.).

Antibodies

The following antibodies were used to detect specific water channel and tight junction proteins: polyclonal rabbit anti-aquaporin-4 antiserum (Chemicon, Hofheim, Germany), monoclonal mouse anti-aquaporin-1 (Acris, Germany), polyclonal rabbit anti-claudin-1 (Zymed, San Francisco, USA), polyclonal rabbit anti-claudin-3 (Zymed, San Francisco, USA), polyclonal rabbit anti-claudin-5 (Liebner et al. 2000), polyclonal rabbit anti-claudin-19 (kindly provided by Mikio Furuse, Kobe, Japan), polyclonal rabbit anti-occludin (Zymed, San Francisco, USA), polyclonal anti-GFAP (DAKO, Hamburg, Germany), monoclonal mouse anti-ZO-1 (Zymed, San Francisco, USA), polyclonal rabbit anti-ZO-1 (Zymed, San Francisco, USA), polyclonal rabbit anti-ZO-2 (Cell Systems, Remagen, Germany), polyclonal rabbit anti-connexin-43 (Sigma, USA). All antisera were used in a dilution of 1:100.

The secondary goat anti-mouse, resp. anti-rabbit antibodies labelled with cyanin-derivative dye Cy3 or Cy2 were purchased from Dianova (Hamburg, Germany). For controls, the primary antibody was omitted. Nuclei were stained with Sytox (green; 1:10,000) or Topro (blue; 1:10,000), both Molecular Probes/Invitrogen, Karlsruhe, Germany.

Immunohistochemistry

Rats were anesthetized and transcardially perfused with 4% paraformaldehyde (PFA). Olfactory epithelium was dissected out and postfixed in 4% PFA in PBS overnight. Subsequently, the tissue was embedded in paraffin and sectioned at 3 µm using a microtome (HM355SS; Micron international, Walldorf, Germany). Sections were placed on Super Frost Plus slides (Micron international, Walldorf, Germany), dewaxed,

and rehydrated by descending alcohol concentrations to aqua dest. For antigen retrieval, they were heated in a steamer in citrate buffer pH 6.0 for 4 min, and finally coated in TBS buffer. To avoid unspecific staining, the sections were blocked by incubation with 5% (w/v) skimmed milk, 0.3% (w/v) Triton X-100 (Serva, Heidelberg, Germany) and 0.4% (w/v) NaN_3 in TBS for 30 min. Primary antibodies diluted in the same solution were applied overnight at 4°C. After three washes in TBS for 10 min, sections were incubated for 45 min with the secondary antibody at room temperature. Following washes in TBS, sections were mounted in Mowiol. Sections were analyzed with a confocal laser scanning microscope (LSM510 META with an Axioplan 2 microscope stand, Zeiss, Göttingen/Jena, Germany) using lasers at 488, 546, and 633 nm for excitation with appropriate filter sets. The system's multi-track function was used to generate images for each stain and excitation sequentially. Images were processed using Adobe Photoshop (version 7.0, Adobe, Mountain View, USA).

Permeability studies

Vascular permeability of the olfactory system was measured by extravasation of the marker fluorescein (MW 376 Da) and Evans blue that binds serum albumin (MW 67 kDa). Under avertin anesthesia rats were given a solution of both dyes (2%, 5 ml/kg) in an injection into the tail vein. After 30 min, the animals were perfused transcardially with 50 ml phosphate-buffered saline for 5 min. The heads were dissected and macroscopic pictures were taken from the head sagittal sections. In case when the permeability of the blood vessels was tested by means of electron microscopy, 1% lanthanum nitrate was added to the fixative, followed by transcardial perfusion (see next paragraph).

Ultrathin section electron microscopy

Rats were transcardially perfused with 2.5% glutaraldehyde (Paesel-Lorei, Frankfurt, Germany) buffered in 0.1 M cacodylate buffer (pH 7.4). Thereafter, the olfactory tissue was dissected out and postfixed in the identical fixative for additional 4 h, and then stored in cacodylate until further processed. The tissues (cerebral cortex, olfactory bulb, nasal mucosa) were postfixed in 1% OsO_4 in 0.1 M cacodylate buffer and then dehydrated in an ethanol series (50, 70, 96, 100%). The 70% ethanol was saturated with uranyl acetate for contrast enhancement. Dehydration was completed in propylene oxide. The specimens were embedded in Araldite (Serva, Heidelberg, Germany). Ultrathin sections were produced on a FCR Reichert Ultracut ultramicrotome (Leica, Bensheim, Germany), mounted on pioloform-coated copper grids, contrasted with lead citrate and analyzed and documented with an EM10A electron microscope (Carl Zeiss, Oberkochen, Germany).

Freeze-fracturing

Olfactory epithelium was dissected out and postfixed with 2.5% glutaraldehyde in 0.1 M cacodylate buffer (pH 7.4) for 2 h at room temperature and stored in cacodylate buffer until used. The tissue was cryoprotected for freeze-fracturing in 30% glycerol and quick-frozen in nitrogen-slush (−210°C). Subsequently, the specimens were fractured in a Balzer`s freeze-fracture device (BAF400D; Balzers, Liechtenstein) at 5×10^{-6} mbar and $^{-}$150°C. The fracture faces were shadowed with platinum/carbon (2 nm, 45°) for contrast and carbon (20 nm, 90°) for stabilization of the replica. After removing the cell material in 12% sodium hypochlorite, the replicas were cleaned several times in double-distilled water and mounted on Pioloform-coated copper grids. The replicas were observed using an EM10A electron microscope (Carl Zeiss, Oberkochen, Germany).

Results

Immunohistochemical stainings

First, we tested the olfactory epithelium and nerve for characteristics of astrocytes, such as the presence of GFAP and aquaporin-4 (AQP4), and for AQP1. Second, we investigated junctional proteins in the olfactory system. A summary of all immunohistochemical staining results performed in this study is given in Table 1.

GFAP The typical marker of astrocytes was tested in the olfactory tissue. Here, the OECs of the olfactory fila were the only cells which showed a positive immunoreactivity for anti-GFAP antibodies (Fig. 1a, b). As a positive control, the olfactory bulb of the same animal was tested for GFAP (data not shown).

Aquaporin-4 The water channel protein AQP4 is the most prominent member of the aquaporin family in the CNS. Due to the common property of OECs and astrocytes to express GFAP, we were particularly interested to find out whether the OECs would also express AQP4. There was clearly no AQP4 reaction on the OECs (Fig. 1c). As a positive control, we investigated the olfactory epithelium on the identical section and found a strong anti-AQP4-staining of basal and supporting cells. In addition, the secretory acinar and duct cells of the Bowman's glands were heavily stained (Fig. 1c).

Aquaporin-1 Endothelial cells in the lamina propria of the olfactory region reacted strongly for AQP1 (Fig. 1d). Moreover, AQP1-antibodies positively labelled perineural cells of the olfactory fila (Fig. 1d). This was supported by

Table 1 Summary of the immunohistochemical findings

	Olf. epithelium	ECs	OECs	Perineural Cells	Bowman's Gland
ZO-1	Sensory cells/supporting cells +++	+++	+++	++	+++
ZO-2	Sensory cells/supporting cells ++ basal cells ++	–	–	–	++
Occludin	Sensory cells/supporting cells +++ whole supporting cells +	+	+++	?	Whole cell +++
Claudin-1	Sensory cells/supporting cells +++	–	–	++	–
Claudin-3	Sensory cells/supporting cells +++	–	–	?	++
Claudin-5	Sensory cells/supporting cells +++	+	++	?	–
Claudin-19	Sensory cells/supporting cells ++	-	-	-	–
GFAP	–	–	+++	–	–
Aquaporin-1	–	+++	–	++	–
Aquaporin-4	Basal and supporting cells +++	–	–	–	+++

double labelling of the perineural cells with the tight junction molecule ZO-1 (Fig. 1d). The olfactory mucosa and the OECs of the olfactory fila were immunonegative for AQP1.

ZO-1 Investigating the classical tight junction protein ZO-1, we found positive reactions to all types of tight junctions in the olfactory epithelium and the lamina propria: In the apical regions of the olfactory epithelium, between the acinar cells and duct cells of Bowman's glands, between endothelial cells of the vessels, perineural cells around the olfactory fila, and between OECs (Figs. 1b–e, 2c–f).

ZO-2 Apical junctions of the olfactory epithelium (between supporting cells and the dendrites of the sensory cells) were heavily labelled by antibodies for the tight junction-associated protein ZO-2, as were the apical junctions of the acinar cells of the Bowman's gland, and endothelial cells (Fig. 1e, arrows). Here, we detected a strong co-labeling with ZO-1 (Fig. 1e). The tight junctions of perineural cells and OECs, positive for ZO-1, were devoid of ZO-2. Interestingly, the basal region of the olfactory epithelium was clearly stained with the anti-ZO-2-antibody, but not with the anti-ZO-1 antibody (Fig. 1e).

Connexin-43 Previously, the gap junction protein connexin-43 had been detected on many cells in the olfactory system (Rash et al. 2005). In our context, we wanted to know whether connexin-43 co-localized with the tight junctions between the OECs. We found clearly spots double labelled for connexin-43 and ZO-1 on the OECs (Fig. 1f). Thus, due to the close co-localization of gap and tight junctions within the fila olfactoria (see below, Fig. 4c), we were not able to decide whether ZO-1 is associated exclusively with tight junctions.

Claudin-1 We tested the olfactory tissues for the presence of claudin-1. Perineural cells around the olfactory fila and the apical tight junctions of the olfactory epithelium between the supporting cells and the sensory cell dendrites stained positive for claudin-1-antibodies. However, the OECs were devoid of any claudin-1 staining (Fig. 2a, b).

Claudin-3 The tight junction protein claudin-3 has been suggested to be a component of blood–brain barrier tight junctions. Accordingly, the endothelial cells in the olfactory bulb were immunopositive for the antibody against claudin-3 as expected (data not shown). In contrast, the endothelial cells within the olfactory lamina propria were negative for claudin-3. OECs and the perineural cells were immunonegative for claudin-3 (Fig. 2c) as well. In the olfactory mucosa, a specific signal could be detected in the olfactory epithelium and in the Bowman's glands (Fig. 2c).

Claudin-5 The occurrence of the endothelial tight junction protein claudin-5 was confirmed in the blood vessels of the olfactory lamina propria. However, the immunoreactivity was rather weak, likely due to the extremely thin walls of the blood vessels in this tissue and rare occurrence of these tight junctions in thin sections (Fig. 2d). Claudin-5 could also be detected both in the apical tight junctions of the olfactory epithelium and in the OECs of the olfactory fila (Fig. 2d).

Claudin-19 The tight junction molecule claudin-19 characteristic for Schwann cells was tested for its presence in OECs. However, claudin-19 immunoreactivity was not found in OECs (Fig. 2e), instead in the apical region of the olfactory epithelium showing tight junctions between supporting cells and the dendrites of the sensory olfactory neurons (Fig. 2e).

Occludin Occludin was the first integral membrane protein of tight junctions detected. For the olfactory system, we confirmed the unambiguously distinct staining of apical olfactory tight junctions (Fig. 2f). For the first time we showed occludin in the fila olfactoria between the OECs (Fig. 2f). Whether or not perineural cells also expressed occludin was not unequivocally clear. Endothelial tight junctions were positively stained as well. Interestingly, in the acinar cells of the Bowman's glands, occludin-specific staining was not restricted to the apical region but spread over most of the cell surface, although the tight junctions

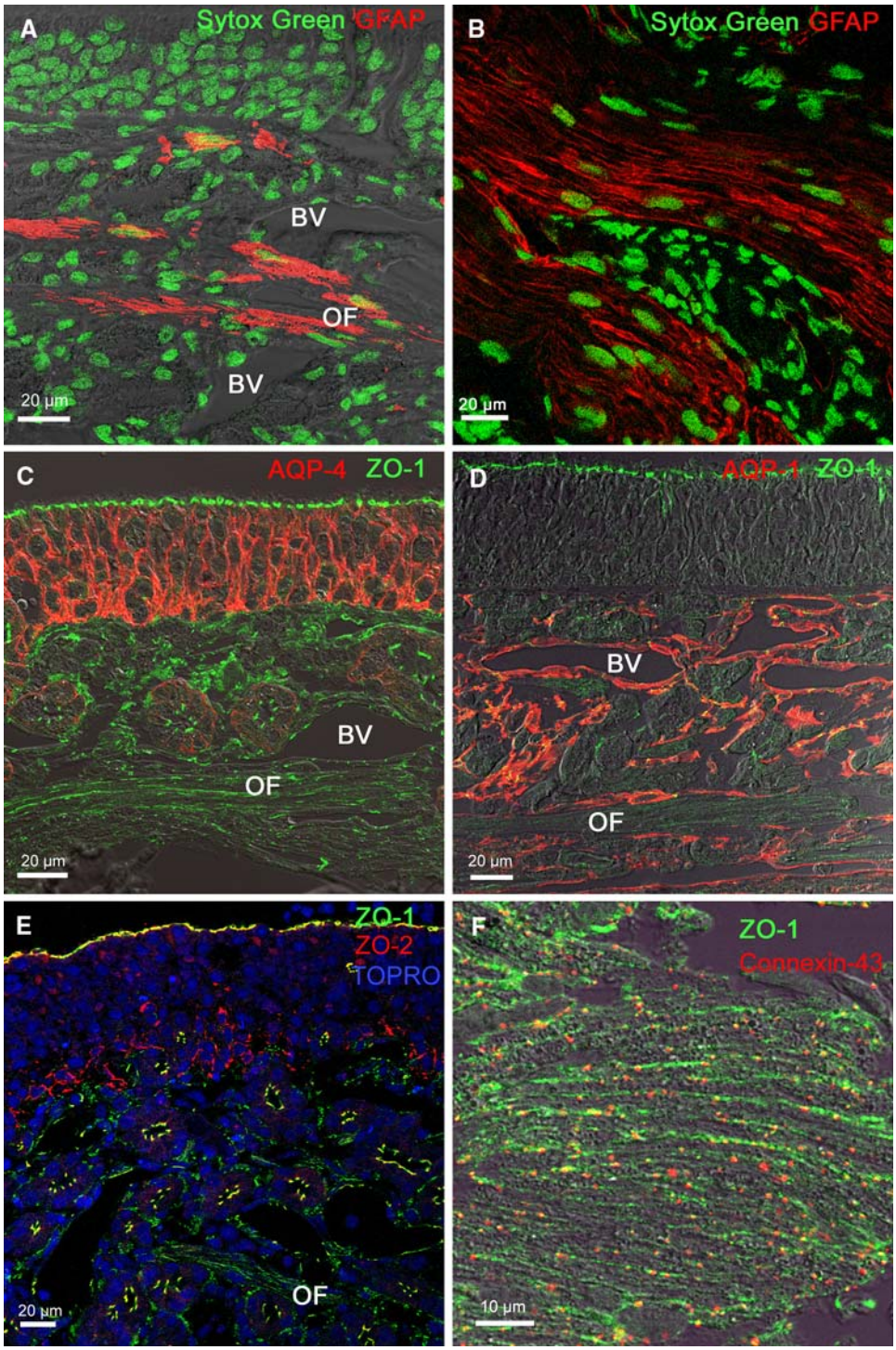

Fig. 1 Immunohistochemical stainings of the peripheral olfactory system (olfactory epithelium and lamina propria with olfactory fila). **a**, **b** Anti-GFAP-staining (*red*) of OECs in an olfactory filum (*OF*) in the lamina propria and shortly before entering the olfactory bulb. *BV* blood vessels. Nuclei are counterstained with Sytox Green (*green*). **c** Double labelling experiment using antibodies against ZO-1 (*green*) and AQP4 (*red*). AQP4 immunoreactivity was seen in the basolateral aspects of the epithelial cells and in the Bowman gland cells. ZO-1 was stained in the apical region of the olfactory epithelium, the Bowman's gland epithelium cells, and the olfactory fila (*OF*). **d** Double labelling experiment using antibodies against ZO-1 (*green*) and AQP1 (*red*). AQP1 heavily stained the endothelial cells within the lamina propria. *BV* blood vessel. **e** Double labelling experiment using antibodies against ZO-1 (*green*) and ZO-2 (*red*). Both molecules were co-localized in the olfactory and the Bowman's gland epithelial cells (merged as *yellow*). The basal cells in the olfactory epithelium were stained selectively by anti-ZO-2 antibody. The OECs in the olfactory fila did not express ZO-2, but ZO-1. **f** Double labelling experiment using antibodies against ZO-1 (*green*) and connexin 43 (*red*) showing gap and tight junctions interconnecting the OECs within the olfactory fila. *Yellow points* mark an overlay of Cx43- and ZO-1-immunoreactivities indicating a close association of gap and tight junctions or a binding of ZO-1 to both gap and tight junction molecules

proper are restricted to the most apical region of the cells shown by anti-ZO-1 staining (Fig. 2f).

Ultrathin section electron microscopy

The ultrastructure of the olfactory epithelium and the lamina propria has been well described previously (for recent articles, see for example Li et al. 2005; Rash et al. 2005). For the purpose of comparison to the other methods applied, it was necessary to briefly delineate the cellular components most important in the context of this study at the ultrastructural level.

The pseudostratified olfactory epithelium was composed of olfactory sensory cells, supporting cells, basal cells, the ducts of the Bowman's glands, and a basal lamina. The lamina propria consisted of three main components (Fig. 3a): the Bowman's glands, the fila olfactoria and two types of blood vessels: capillaries with thin endothelial

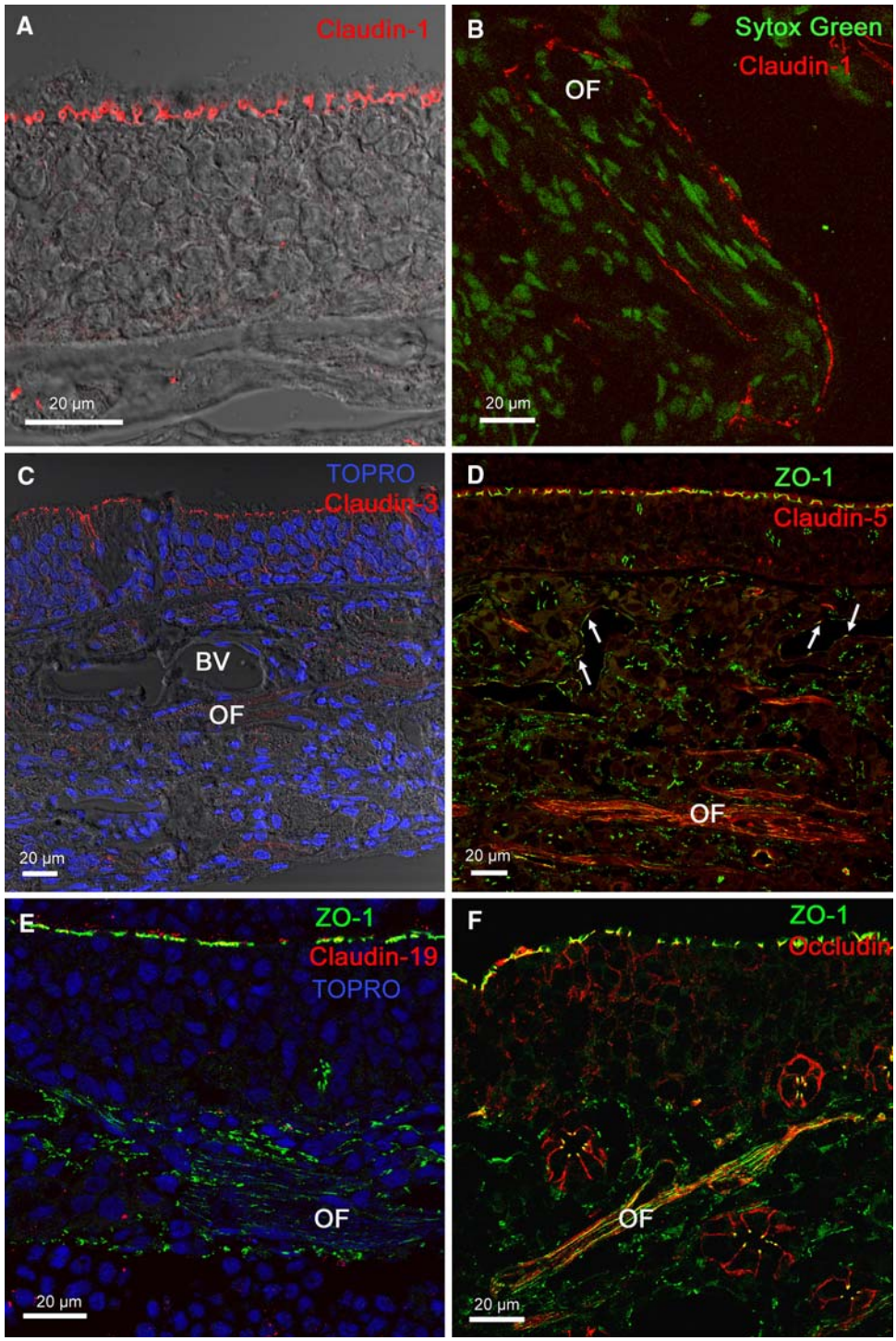

Fig. 2 Immunohistochemical stainings of the peripheral olfactory system [olfactory epithelium and lamina propria with olfactory fila (*OF*)]. **a**, **b** Anti-claudin-1 staining (*red*) of the apical tight junctions between supporting cells and dendrites of the sensory epithelial cells **a**, and perineural cells **b**. The OECs were immunonegative for claudin-1. **C.** Labelling experiment using an antibody against claudin-3 (*red*). Claudin-3 stains the apical tight junctions in the olfactory epithelium and the Bowman's gland epithelial cells. Importantly, the blood vessel (*BV*) endothelial cells were not immunoreactive for claudin-3. **d** Double labelling experiment using antibodies against ZO-1 (*green*) and claudin-5 (*red*). Whereas the claudin-5 immunoreactivity was difficult to detect in vascular endothelial cells (*arrows*), it could easily be found in the olfactory fila. In addition, the apical tight junctions of the olfactory epithelium were also positively stained with the anti-claudin-5 antibody, seen as overlapping staining with ZO-1. **e** Double labelling experiment using antibodies against ZO-1 (*green*) and claudin-19 (*red*). Olfactory ensheathing cells were negative for claudin-19; however, apical tight junctions of the olfactory epithelium were immunoreactive against claudin-19. **f** Double labelling experiment using antibodies against ZO-1 (*green*) and occludin (*red*). Again, both molecules are co-localized in the olfactory and the Bowman's gland epithelial cells (merged as *yellow*). In addition, occludin stains the entire surface of Bowman's glandular cells, and, more weakly, the basolateral membranes of the olfactory epithelium

cells and venules or arterioles with smooth muscle cells adjacent to endothelial cells. The fila olfactoria consisted of bundles of very small axons (diameter in the order of 0.1–0.2 µm), which were surrounded by thin, slender processes of OECs whose nuclei are predominantly located at the margin of a filum (Fig. 3b). The OECs were interconnected by gap and tight junctions (Fig. 3c), which were found mainly at the margin of a filum, but occasionally also in the center of a filum. Sometimes, it was impossible to differentiate between gap and tight junctions (see description of immunohistochemistry, Fig. 2f, and of freeze-fracture replicas, Fig. 4c). At some places, OECs were found forming slender processes with an enormously enlarged surface (Fig. 3d). Only few axons were found in these OEC-rich compartments, confirming that these structures were olfactory fila. Possibly, these curious cellular surface

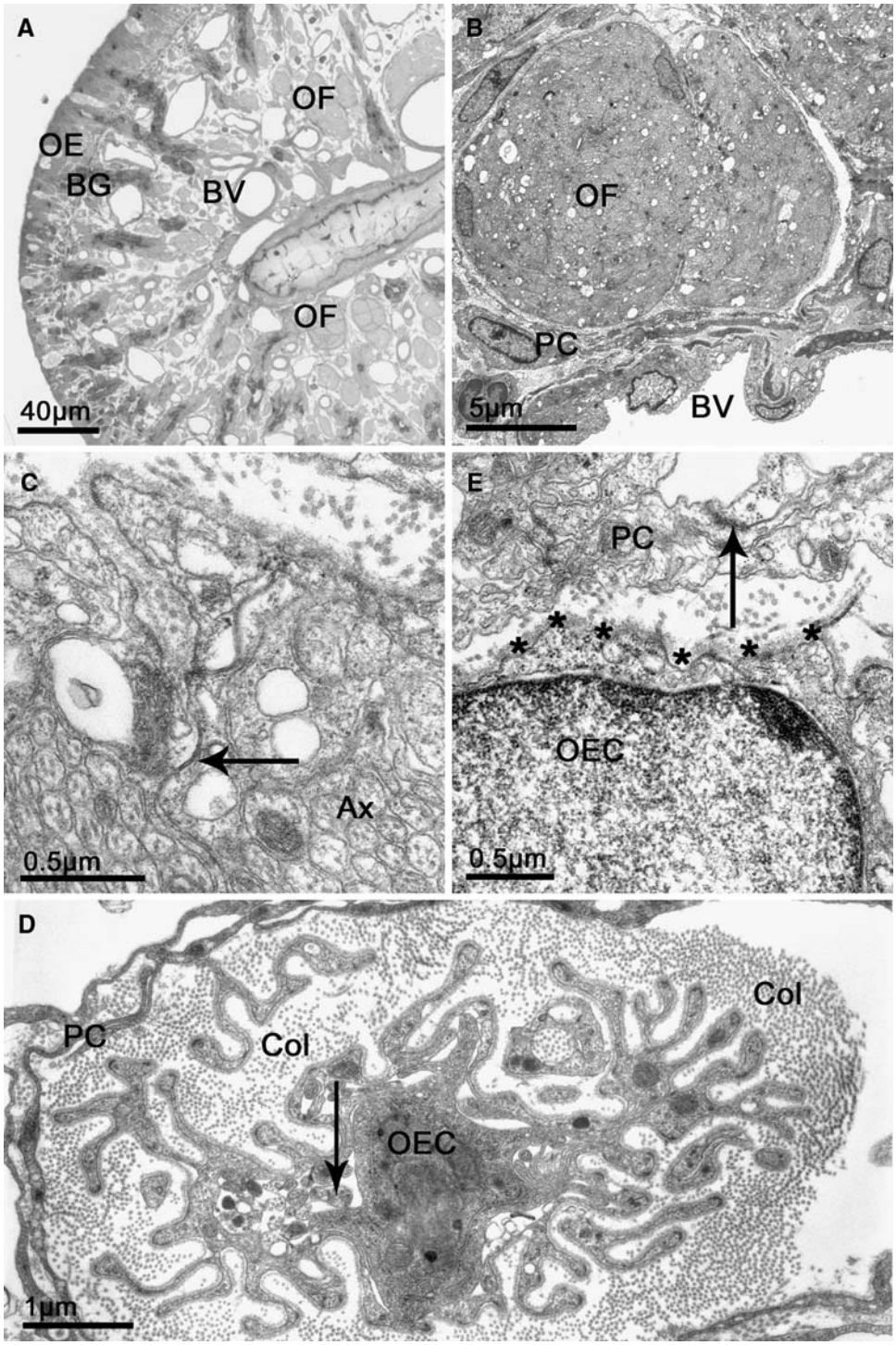

Fig. 3 Light and electron microscopy of the olfactory system of the rat. **a** Semithin section through the olfactory epithelium and the lamina propria. *OE* olfactory epithelium, *OF* olfactory filum surrounding bundles of olfactory axons, BG Bowman's gland, *BV* blood vessel. **b** Ultrathin section through an olfactory filum (*OF*) adjacent to a blood vessel (*BV*). In between both structures, perineural cells (*PC*) surrounded the olfactory filum. **c** Ultrathin section through an olfactory filum at higher magnification. *Ax* olfactory axons, the *arrow* labels a tight junction between two olfactory ensheathing cells or cell processes. **d** Ultrathin section through an olfactory filum showing perineural cells (*PC*) interconnected by tight junctions (*arrow*) beneath an olfactory ensheathing cell (*OEC*) covered by a basal lamina (*asterisks*). **e** Olfactory filum with an extremely small number of axons (*arrow*), but a highly increased surface of the olfactory ensheathing cell (*OEC*). Col collagen between the olfactory filum and the associated perineural cell (*PC*)

formations were a morphological expression of the high dynamics of generation and growth of olfactory sensory neurons and their axons. Beneath the basal lamina, the fila olfactoria were surrounded by another cell type interconnected by tight junctions as well, the perineural cells (Fig. 3e). Although consistently found surrounding the olfactory fila, these cells formed a discontinuous rather than a continuous tube around each filum. The perineural sheath accompanied the olfactory fila up to the entry into the olfactory bulb where it continued as meningeal sheath of the pia mater of the brain (data not shown).

Freeze-fracture electron microscopy

The knowledge of the ultrathin section-derived morphology of the olfactory mucosa was absolutely necessary for the

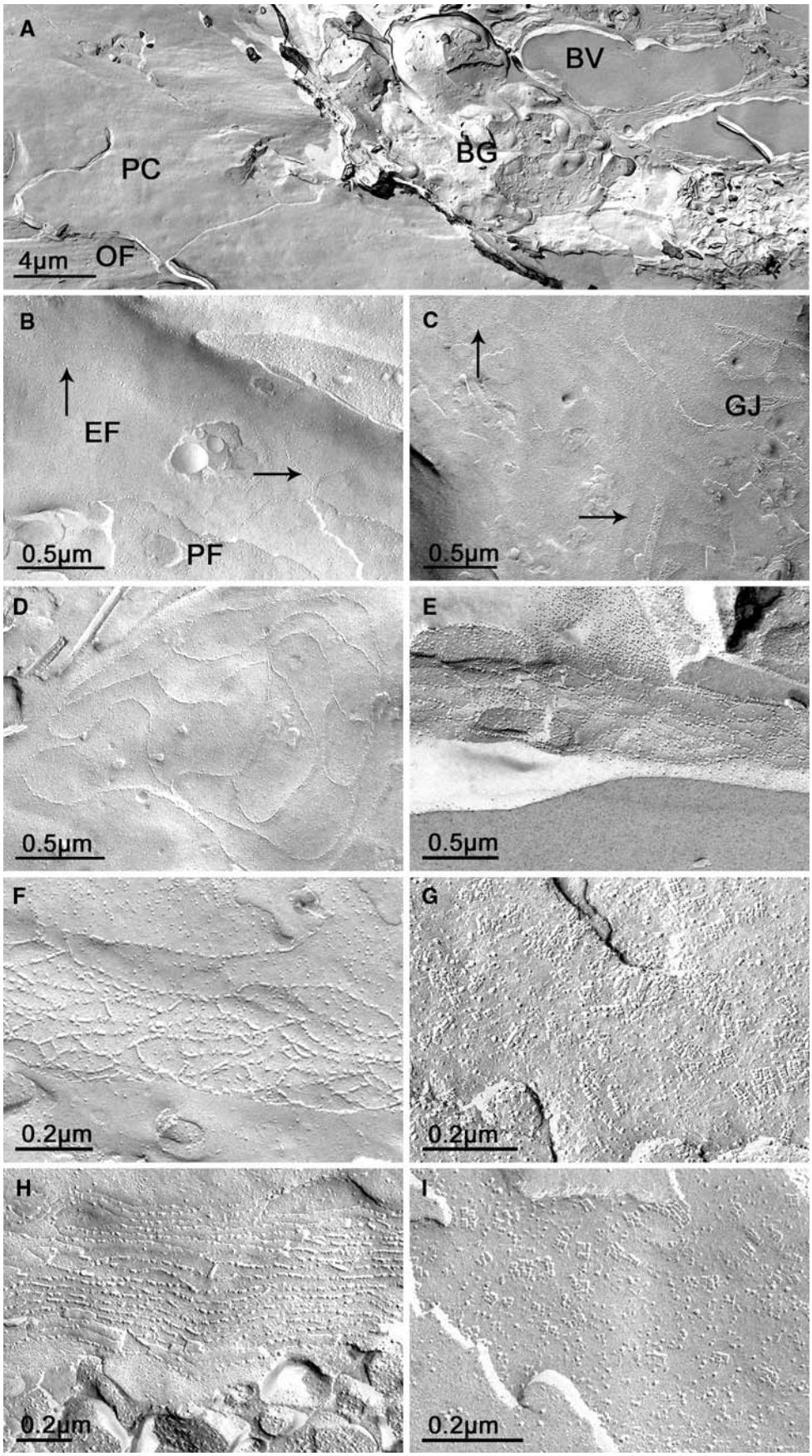

Fig. 4 Freeze-fracture replicas of the olfactory system of the rat. **a** Overview of a typical freeze-fracture replica of the lamina propria of the olfactory system. *PC* perineural cells, covering an olfactory filum (*OF*) *BG* Bowman's gland, *BV* blood vessel. **b**, **c**. Freeze-fracture replicas of tight and gap junctions (*GJ*) of the olfactory ensheathing cells. *EF* external fracture face, *PF* protoplasmic fracture face. In **b**, *arrows* label E-face associated tight junctional particles, in **c,** P-face associated tight junctional ridges poorly occupied by particles. **d** Tight junctions of perineural cells at the P-face. **e** Tight junctions of blood vessel endothelial cells densely meshed and mostly associated with the E-face. **f** Tight junctions of the Bowman's gland epithelial cells, mostly associated with the P-face. **g** Basolateral membranes of Bowman's gland epithelial cells revealed a high number of orthogonal arrays of particles. **h** Tight junctions between olfactory sensory cells or olfactory sensory cells and supporting cells. Again, the strands are mainly associated with the P-face, but less meshed and more arranged in parallel orientation. i As shown in **g**, the basolateral membranes of olfactory sensory and/or supporting cells revealed a high number of orthogonal arrays of particles

interpretation of the appropriate freeze-fracture replicas. Figure 4a shows an overview of a replica containing most of the relevant cells observed in this study. To our knowledge, there is no other previously published study describing such an enormous diversity of tight junctions in terms of molecular composition and morphological heterogeneity as in the olfactory system. Most easily, we could recognize the fila olfactoria. In association with olfactory fibers, we identified OEC membranes and confirmed the absence of OAPs and presence of tight junctions, as reported previously (Mack and Wolburg 1986; Fig. 4b). These tight junctions were relatively poorly meshed and incompletely occupied by tight junction particles, mostly associated with the E-face (Fig. 4b). At some places, gap junctions could be observed together with tight junctions: here, the P-face-associated connexons were longitudinally arranged within the framework of tight junctional strands, which revealed only ridges very poor in particles at the P-face (Fig. 4c). This explained why it was sometimes impossible to differentiate between gap and tight junctions in ultrathin sections. If perineural cell membranes were freeze-fractured, they revealed large planes, with local exposition of smoothly curved and poorly meshed tight junctions predominantly associated with the P-face (Fig. 4d). The overall insertion of particles within the tight junctional ridges was even more complete than in the OEC tight junctions. An additional type of tight junction was found between the endothelial cells. This type is first of all characterized by a high degree of complexity of the strands and a high degree of E-face-association (Fig. 4e). The tight junctions of Bowman's gland epithelial cells were similarly complex as the endothelial tight junctions, but mainly associated with the P-face (Fig. 4f). Interestingly, the basolateral membranes of Bowman's gland epithelial cells were packed with a lot of OAPs (Fig. 4g). Thus, in the case of an epithelial glandular cell, OAPs and tight junctions co-localized in the same cytoplasmic membrane. This finding correlated well with the positive immunoreactivity for aquaporin-4 (Fig. 1c). The same situation was found in the olfactory (sensory) epithelial cells interconnected by tight junctions with poorly intermeshed and parallel strands (Fig. 4h). These cells also contained OAPs in their basolateral membranes (Fig. 4i) which correlated with the immunoreactivity against aquaporin-4 (Fig. 1c).

Evan's blue and Lanthanum labelling

In order to test the permeability of blood vessels in the olfactory system, we injected Evan's blue and fluorescein dyes intravenously or perfused the rat transcardially with glutaraldehyde containing 1% lanthanum nitrate. The marker dyes leaked out of blood vessels in the entire olfactory system. Evan's blue stained the tissue green, whereas the brain remained unstained (Fig. 5). Lanthanum nitrate could easily be detected in the electron microscope as a black precipitate and allowed us to distinguish between tracer penetrating the interendothelial cleft or being transported through the endothelial cells via endocytosis.

As expected, the blood vessels within both, the cerebral cortex (Fig. 6a, b) and the olfactory bulb (Fig. 6c, d) were tight for lanthanum. The tracer diffused only a small distance between the cells, approximately of 0.5–1 µm, and then abruptly stopped where the tight junction obstructed the way. The subendothelial space, in particular the basal lamina, was devoid of any tracer particles (Fig. 6a–d).

In clear contrast, the blood vessels of the olfactory lamina propria of the same animal were leaky: the lanthanum had travelled through the entire interendothelial cleft and labelled the subendothelial space (Fig. 6e). Both the subendothelial basal lamina and the basal lamina around the olfactory fila were labelled, demonstrating that the tight junctions were not able to obstruct the paracellular passage between the endothelial cells. The lanthanum that had leaked through not only labelled the subendothelial basal lamina, but also the basal lamina covering the OECs (see large arrow in Fig. 6f). Indeed, the labelling of the surface of fila olfactoria showed the leakage of tracer through the perineural sheath raising the question of the function of perineural tight junctions. Even the fila olfactoria were poorly labelled and not consistently empty of lanthanum staining

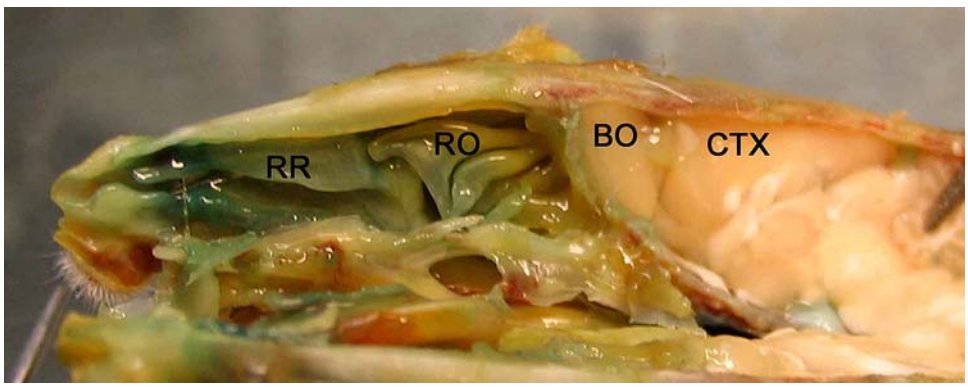

Fig. 5 Macroscopical aspect of the rat brain after injection of Evan's blue into the tail vein. As can clearly be seen, both the respiratory (*RR*) as well as the olfactory region (*OR*) of the nasal cavity were stained green-blue, directly showing the high permeability of the blood vessels in this region of the olfactory system. In contrast, the brain (cortex, *CTX)* including the olfactory bulb (*BO*) remained unstained

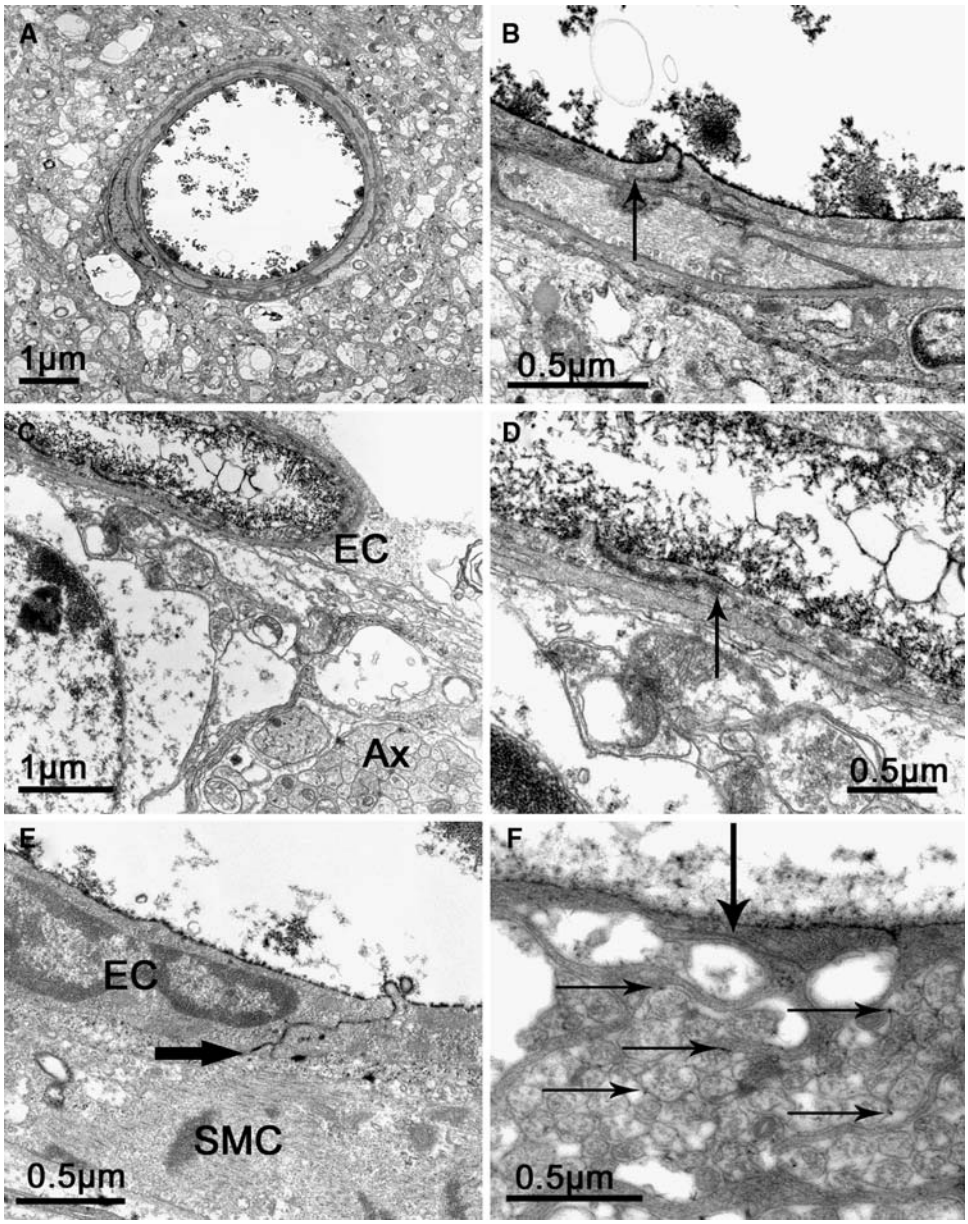

Fig. 6 Lanthanum labelling after transcardial perfusion of lanthanum nitrate together with the fixative. **a**, **b** Analysis of the lanthanum distribution in cortical vessels at low (**a**) and higher (**b**) magnification. The *arrow* in **b** shows the stop of lanthanum penetrating the interendothelial cleft: the subendothelial space was unstained and clean of lanthanum. **c**, **d** The same experiment as shown in **a**, **b** in the olfactory bulb. In **c**, olfactory axons (*Ax*) running into the olfactory bulb were located near a blood vessel. This vessel is tight as shown by restriction of lanthanum penetration within the interendothelial cleft. **e** Analysis of the lanthanum distribution in the lamina propria of the olfactory system. The interendothelial cleft was open indicated by lanthanum deposits down to the subendothelial space (*arrow*). *EC* endothelial cell, *SMC* smooth muscle cell. **f** Analysis of the lanthanum distribution in an olfactory filum. The basal lamina surrounding the filum (*top*) was labelled by numerous lanthanum deposits. The large arrow points to a tight junction interconnecting two processes of an olfactory ensheathing cell. Within the filum and between the axons, very small deposits of lanthanum could be found demonstrating transfer of lanthanum from the interstitial to the periaxonal space (*horizontal arrows*)

(Fig. 6f) suggesting that the tight junctions of OECs were able to hinder but not to obstruct completely the penetration of tracer into the fila olfactoria.

Discussion

In the present study, we investigated the expression pattern of water channel proteins as well as tight junctional proteins in the olfactory system of the rat and compared these features with permeability properties of the vascular system. The intent of this study was to present morphological data important to address questions regarding the role of the neurovascular unit within the olfactory system. These questions are particularly relevant in the context of axonal growth, vascular permeability and the putative role of interglial connectivity.

Axonal growth and the neurovascular unit

An important reason moving the olfactory system into the centre of scientific awareness was the ability of the olfactory ensheathing (glial) cells (OECs) to support axonal growth after transplantation into spinal cord lesions (see, for example, Li et al. 1997, 2005; Imaizumi et al. 2000; Raisman 2001; Barnett and Chang 2004; López-Vales et al. 2007). In remarkable contrast to these successful efforts to elucidate functional aspects sensory olfactory neurons and

OECs, relatively little is known about cellular interactions within the olfactory system, in particular the interactions between OECs, axons and vascular structures. The concept of the so-called neurovascular unit describing complex interrelationships between neurons, glial cells and microvessels (Iadecola 2004; Simard and Nedergaard 2004) has never been applied to the olfactory system. Recently, several studies have been published focussing on junctional connections in the olfactory epithelium (Menco 1988; Miragall et al. 1994; Hussar et al. 2002; Rash et al. 2005; Ablimit et al. 2006), but only little attention has been paid to the cellular system of the olfactory fila.

Interglial connectivity

Mack and Wolburg (1986) have been the first to describe tight junctions between OECs in the rat olfactory system, and Miragall et al. (1994) detected expression of the tight junction molecule ZO-1 in the olfactory fila. Wolburg and Kästner (1984) for the first time suggested a relationship between tight junction-linked astroglial cells and their growth promoting ability in certain fibre tracts among vertebrates. This hypothesis has recently found support by the observation that newly grown retinal ganglion cell axons are guided within the fish optic nerve by astrocytes interconnected by claudin-1-based tight junctions (Mack and Wolburg 2006). This prompted us to test the occurrence of claudin-1 in OEC tight junctions. However, the OECs turned out to be immunonegative for claudin-1, whereas the perineural cells and the apical tight junctions between supportive and sensory cells in the olfactory epithelium were found to be immunopositive for claudin-1 (Fig. 2a, b; see Table 1).

The reason for testing claudin-19 in the olfactory system was the hypothesis of Wewetzer et al. (2002) that all OECs are Schwann cells which develop their characteristic phenotype under the specific influence of the olfactory system. In this view, the absence of the Schwann cell-specific claudin-19 (Miyamoto et al. 2005) reflects a suppression of this phenotype in the olfactory environment (Fig. 2e). It remains to be tested whether OECs isolated from the influence of the olfactory system by disintegration of the neuron/OEC unit, would upregulate claudin-19. As a by-product of this investigation, we detected claudin-19 immunoreactivity in tight junctions between supporting cells and the dendrites of the sensory olfactory neurons. Thus, the tight junctions characterized first of all by a dense pattern of parallel strands (Fig. 4h) may consist of claudin-19, besides claudin-3 (Fig. 2c), claudin-5 (Fig. 2d), occludin (Fig. 2f) and ZO1/2 (Fig. 1e).

Interestingly, the axons of olfactory neurons run in bundles wrapped by OEC processes, yet without any glial separation of individual axons. This has prompted investigations suggesting ephaptic interactions between adjacent axons (Bokil et al. 2001; Blinder et al. 2003). Thus, tight junctions between OEC processes might serve to confine interactions between axons. Obviously, to this end complete physiological tightness of the tight junctions seems not no be needed (Fig. 6f).

The putative mechanism of how interglial tight junctions could support axonal growth and/or regeneration is completely unknown. Nevertheless, it seems plausible that tight junctions contribute to a micro-compartmentalization in the appropriate fibre tract which is not only compatible with, but even actively stimulates axonal growth.

Axonal growth and vascular permeability

It is plausible that the composition of a supportive microenvironment needs access to the blood vessels which then should be devoid of a strict blood–tissue barrier. The mechanism of how tight junctions might enable axons to grow remains poorly understood. Nevertheless, tight junctions between astrocytes or OECs could be responsible for the establishment of tiny extracellular compartments leading to a microenvironment which supports axonal growth (Wolburg and Kästner 1984; Mack and Wolburg 1986, 2006). Composing a supportive microenvironment should imply access to blood-borne substances and thus leakage through blood vessels. In fact, there are several reports raising the issue of a relationship between compromised blood–brain barrier properties and regenerative capability (Risling et al. 1989, 1993; Lorenzo 1992; Xiang et al. 2005; Pan et al. 2006).

In the present study, we demonstrate for the first time that the blood vessels of the lamina propria of the olfactory mucosa are leaky for perfused lanthanum nitrate as an accepted electron microscopical tracer. However, to protect the olfactory axons from the full spectrum of blood-borne substances, many being neurotoxic, the tight junctions of the OECs are necessary to filter those compounds favourably for growing axons. In any case, the OEC tight junctions form a barrier for lanthanum nitrate, which nevertheless is incomplete allowing a low amount of leakage from the interstitial to the periaxonal space (Fig. 6f). Interestingly, the tight junctions in the OECs, perineural cells and endothelial cells differ in their molecular composition and freeze-fracture morphology. For example, claudin-3 has been referred to as a key molecule of the blood–brain barrier tight junctions to be responsible for tightness (Wolburg et al. 2003). Claudin-3 was not detectable in the blood vessels of the olfactory lamina propria (Fig. 2c). The tight junction molecule claudin-5 is believed to be characteristic for endothelial cells (Morita et al. 1999). There has hitherto been one exception from the rule of endothelial expression of claudin-5, namely the expression by gastrointestinal epithelial cells (Rahner et al. 2001). In this study,

we found claudin-5 in endothelial cells and in the OECs as well (Fig. 2d). This finding may support doubts that claudins are expressed in a strictly cell-specific manner. However, the mechanism for insertion in the plasma membrane seems to be specific for a given claudin: in accordance with a previous report (Morita et al. 1999), the claudin-5-positive tight junctions of the OECs were predominantly associated with the E-face (Fig. 4b).

Tight junctions, OAPs, and aquaporins

The finding that glial cells which form tight junctions do not possess any OAPs, or form OAPs but no tight junctions, lead to the hypothesis of mutual exclusiveness of both structures (Mack et al. 1987). Indeed, the OECs have tight junctions and no OAPs, astrocytes at least of mammals have OAPs and no tight junctions. The reason for this mutual exclusiveness is not clear and biochemically and functionally unknown, except that both structures are involved in the regulation of liquid flow. Since OAPs are now known to contain aquaporin-4 (AQP4; for a review, see, for example, Wolburg 2006), it seemed probable that OECs would not express AQP4. This expectation was confirmed in this study (Fig. 1c). Nevertheless, an exception from the rule of mutual exclusiveness of OAPs/AQP4 and tight junctions was found in the olfactory sensory cells and acinar cells of the Bowman's gland. OAPs in sensory olfactory neurons have already been described by Miragall (1983). We found both, a strong immunoreactivity for AQP4, OAPs and tight junctions in the membranes of these cells. Moreover, in the freeze-fracture replica of Bowman's gland cells, the tight junctions were elaborate structures, highly associated with the P-face and highly meshed (Fig. 4f). The immunohistochemical stainings including double labelling experiments showed that the tight junctions contained at least ZO-1, ZO-2, and occludin. The anti-claudin-3 antibody gave a weak signal, and other claudins such claudin-2 or claudin-4 were not tested. Surprisingly, occludin was distributed across the entire surface of the cells. To our knowledge, this is the first report concerned with insertion of the tight junction molecule occludin outside of epithelial tight junctions. In experiments addressing formation of tight junctions introducing point mutations into the second extracellular loop of claudin-5, a so-called disjunction type was defined as characterized by targeting to the plasma membrane but not restricting to the junction domain (Piontek et al. 2008). However, it is not clear if the presence of occludin in the Bowman's gland and olfactory epithelial cell outside the tight junction may be caused by a similar alteration. If so, this would mean that occludin would fulfil other tasks outside the tight junctions, and that this non-junctional function would be associated with an altered primary structure of the extracellular loop(s).

Another important water channel protein, AQP1, has been originally detected in erythrocytes and since then described in many tissues, including kidney, secretory and absorptive epithelia, gall bladder, portions of the male reproductive system (for reviews, see Verkman 2002; King et al. 2004), choroid plexus (Speake et al. 2003), endothelial cells in the kidney (Nielsen et al. 1993), and in carcinomas and glioblastomas (Endo et al. 1999). In the olfactory system, perineural cells around the fila olfactoria were found to be highly immunoreactive for anti-AQP1 antibodies (Ablimit et al. 2006; this study, Fig. 1d), the OECs were immunonegative. However, endothelial cells showed the strongest immunoreactivity for AQP1. Endothelial expression of AQP1 is controversially discussed in the literature (Endo et al. 1999). There seems to be a large variability between different vascular beds. For example, it has been discussed whether fenestration of capillaries would be connected to AQP1 expression (Maunsbach et al. 1997). However, in the choroid plexus, only the epithelial cells express AQP1 and not the fenestrated capillaries beneath (Mack and Wolburg, unpublished observations). Therefore, the strong expression of AQP1 by olfactory blood vessels seems to be a specific for this tissue the functional relevance of which is not understood so far.

Conclusions

The observation that the OECs are interconnected by tight junctions has been suggested to be relevant for regenerative processes, because tight junction-connected glial cells could contribute to a growth-supportive environment. However, we are aware of the absence of any direct experimental evidence in favour of a causal relationship between interglial connectivity and axonal growth promotion. Immunocytochemistry and freeze-fracturing supported the hypothesis that tight junctions and AQP4-positive OAPs are mutually exclusive as has been described previously for glial cells. In OECs, we found neither OAPs nor AQP4, but tight junctions which were immunoreactive for ZO-1, occludin and claudin-5, but immunonegative for ZO-2 and claudin-3. The permeability and tight junction composition of blood vessels showed that they were permeable for lanthanum nitrate and to be immunopositive for ZO-1 and claudin-5, but not claudin-3 as was the case for tight (blood–brain barrier) vessels in the olfactory bulb. Further experiments are needed to test the idea that the tight junctions of the OECs are necessary to restrict the whole of blood-borne substances and to filter those providing a benefit for axonal growth.

Acknowledgments This study was supported by a grant of the Hertie-foundation (grant number 1.01.1/07/003) to HW and KW-B. The skilful technical assistance of A. Adam (immunohistochemistry), E.-M. Knittel (freeze-fracturing), and G. Frommer-Kästle (ultrathin sections) is gratefully acknowledged.

References

Ablimit A, Matsuzaki T, Tajika Y, Aoki T, Hagiwara H, Takata K (2006) Immunolocalization of water channel aquaporins in the nasal olfactory mucosa. Arch Histol Cytol 69:1–12

Barnett SC, Chang L (2004) Olfactory ensheathing cells and CNS repair: going solo or in need of a friend? Trends Neurosci 27:54–60

Blinder KJ, Pumplin DW, Paul DL, Keller A (2003) Intercellular interactions in the mammalian olfactory nerve. J Comp Neurol 466:230–239

Bock P, Beineke A, Techangamsuwan S, Baumgärtner W, Wewetzer K (2007) Differential expression of HNK-1 and $p75^{NTR}$ in adult canine Schwann cells and olfactory ensheathing cells in situ but not in vitro. J Comp Neurol 505:572–585

Bokil H, Laaris N, Blinder K, Ennis M, Keller A (2001) Ephaptic interactions in the mammalian olfactory system. J Neurosci 21:173RC (1–5)

Dermietzel R (1973) Visualization by freeze-fracturing of regular structures in glial cell membranes. Naturwissenschaften 60:208

Endo M, Jain RK, Witwer B, Brown D (1999) Water channel (aquaporin-1) expression and distribution in mammary carcinomas and glioblastomas. Microvasc Res 58:89–98

Graziadei PP, Monti Graziadei GA (1985) Neurogenesis and plasticity of the olfactory sensory neurons. Ann NY Acad 457:127–142

Hussar P, Tserentsoodol N, Koyama H, Yokoo-Sugawara M, Matsuzaki T, Takami S, Takata K (2002) The glucose transporter GLUT1 and the tight junction protein occludin in nasal olfactory mucosa. Chem Senses 27:7–11

Iadecola C (2004) Neurovascular regulation in the normal brain and in Alzheimer's disease. Nature Rev Neurosci 5:347–360

Imaizumi T, Lankford KL, Burton WV, Fodor WL, Kocsis JD (2000) Xenotransplantation of transgenic pig olfactory ensheathing cells promotes axonal regeneration in rat spinal cord. Nature Biotech 18:949–953

Jessen KR, Mirsky R (2005) The origin and development of glial cells in peripheral nerves. Nature Rev Neurosci 6:671–682

King LS, Kozono D, Agre P (2004) From structure to disease: the evolving tale of aquaporin biology. Nature Rev Mol Cell Biol 5:687–698

Li Y, Field PM, Raisman G (1997) Repair of adult rat corticospinal tract by transplants of olfactory ensheathing cells. Science 277:2000–2002

Li Y, Field PM, Raisman G (2005) Olfactory ensheathing cells and olfactory nerve fibroblasts maintain continuous open channels for regrowth of olfactory nerve fibres. Glia 52:245–251

Liebner S, Fischmann A, Rascher G, Duffner F, Grote E-H, Kalbacher H, Wolburg H (2000) Claudin-1 expression and tight junction morphology are altered in blood vessels of human glioblastoma multiforme. Acta Neuropathol 100:323–331

López-Vales R, Forés J , Navarro X, Verdú E (2007) Chronic transplantation of olfactory ensheathing cells promotes partial recovery after complete spinal cord transection in the rat. Glia 55:303–311

Lorenzo A (1992) Ultrastructural observations on blood vessels surrounding normal and regenerating spinal cord in newt. Ital J Anat Embryol 97:257–272

Mack A, Wolburg H (1986) Heterogeneity of glial membranes in the rat olfactory system as revealed by freeze-fracturing. Neurosci Lett 65:17–22

Mack A, Neuhaus J, Wolburg H (1987) Particular relationship between orthogonal arrays of particles and tight junctions as demonstrated in cells of the ventricular wall of the rat brain. Cell Tissue Res 248:619–625

Mack A F, Wolburg H (2006) Growing axons in fish optic nerve are accompanied by astrocytes interconnected by tight junctions. Brain Res 1103:25–31

Mackay-Sim A, Kittel P (1991) Cell dynamics in the adult mouse olfactory epithelium: a quantitative autoradiographic study. J Neurosci 11:979–984

Maunsbach AB, Marples D, Chin E, Ning G, Bondy C, Agre P, Nielsen S (1997) Aquaporin-1 water channel expression in human kidney. J Am Soc Nephrol 8:1–14

Menco BP (1988) Tight-junctional strands first appear in regions where three cells meet in differentiating olfactory epithelium: a freeze-fracture study. J Cell Sci 89:495–505

Miragall F (1983) Evidence for orthogonal arrays of particles in the plasma membranes of olfactory and vomeronasal sensory neurons of vertebrates. J Neurocytol 12:567–576

Miragall F, Krause D, De Vries U, Dermietzel R (1994) Expression of the tight junction protein ZO-1 in the olfactory system: presence of ZO-1 on olfactory sensory neurons and glial cells. J Comp Neurol 341:433–448

Miyamoto T, Morita K, Takemoto D, Takeuchi K, Kitano Y, Miyakawa T, Nakayama K, Okamura Y, Sasaki H, Miyachi Y, Furuse M, Tsukita S (2005) Tight junctions in Schwann cells of peripheral myelinated axons: a lesson from claudin-19-deficient mice. J Cell Biol 169:527–538

Morita K, Sasaki H, Furuse M, Tsukita S (1999) Endothelial claudin: claudin-5/TMVCF constitutes tight junction strands in endothelial cells. J Cell Biol 147:185–194

Nielsen S, Smith BL, Christensen EI, Agre P (1993) Distribution of the aquaporin CHIP in secretory and resorptive epithelial and capillary endothelia. Proc Natl Acad Sci USA 90:7275–7279

Pan W, Cain C, Yu Y, Kastin AJ (2006) Receptor-mediated transport of LIF across blood–spinal ciord barrier is upregulated after spinal cord injury. J Neuroimmunol 174:119–125

Piontek J, Winkler L, Wolburg H, Müller SL, Zuleger N, Piehl C, Wiesner B, Krause G, Blasig IE (2008) Formation of tight junction: determinants of homophilic interaction between classic claudins. FASEB J 22:146–158

Raisman G (2001) Olfactory ensheathing cells—another miracle cure for spinal cord injury? Nature Rev Neurosci 2:369–375

Rahner C, Mitic LL, Anderson JM (2001) Heterogeneity in expression and subcellular localization of claudins 2, 3, 4, and 5 in the rat liver, pancreas, and gut. Gastroeneterology 120:411–422

Ramón-Cueto A, Avila J (1998) Olfactory ensheathing glia: properties and function. Brain Res Bull 46:175–187

Rash JE, Davidson KGV, Yasumura T, Furman CS (2004) Freeze-fracture and immunogold analysis of aquaporin-4 (AQP4) square arrays, with models of AQP4 lattice assembly. Neuroscience 129:915–934

Rash JE, Davidson KGV, Kamasawa N, Yasumura T, Kawasama M, Zhang C, Michaels R, Restrepo D, Ottersen OP, Olson CO, Nagy JI (2005) Ultrastructural localization of connexins (Cx36, Cx43, Cx45), glutamate receptors and aquaporin-4 in rodent olfactory mucosa, olfactory nerve and olfactory bulb. J Neurocytol 34:307–341

Risling M, Lindao H, Cullheim S, Franson P (1989) A persistent defect in the blood–brain barrier after ventral funiculus lesion in adult cats: implications for CNS regeneration? Brain Res 494:13–21

Risling M, Fried K, Lindå H, Carlstedt T, Cullheim S (1993) Regrowth of motor axons following spinal cord lesions: distribution of laminin and collagen in the CNS scar tissue. Brain Res Bull 30:405–414

Simard M, Nedergaard M (2004) The neurobiology of glia in the context of water and water homeostasis. Neuroscience 129:877–896

Speake T, Freeman LJ, Brown PD (2003) Expression of aquaporin 1 and aquaporin 4 water channels in rat choroid plexus. Biochim Biophys Acta 1609:80–86

Verkman AS (2002) Aquaporin water channels and endothelial cell function. J Anat 200:617–627

Wewetzer K, Verdu E, Angelov DN, Navarro X (2002) Olfactory ensheathing glia and Schwann cells: two of a kind? Cell Tissue Res 309:337–45

Wolburg H (1995) Orthogonal arrays of intramembranous particles: a review with special reference to astrocytes. J Brain Res 36:239–258

Wolburg H (2006) The endothelial frontier. In: Dermietzel R, Spray DC, Nedergaard M (eds) Blood–brain barriers. From ontogeny to artificial interfaces. Wiley-VCH Weinheim pp 77–107

Wolburg H, Kästner R (1984) Astroglial–axonal interrelationship during regeneration of the optic nerve in goldfish. J Hirnforsch 25:493–504

Wolburg H, Kästner R, Kurz-Isler G (1983) Lack of orthogonal particle assemblies and presence of tight junctions in astrocytes of the goldfish (*Carassius auratus*). A freeze-fracture study. Cell Tissue Res 234:389–402

Wolburg H, Neuhaus J, Mack A (1986) The glio-axonal interaction and the problem of regeneration of axons in the central nervous system–concept and perspectives. Z Naturforsch 41c:1147–1155

Wolburg H, Wolburg-Buchholz K, Kraus J, Rascher-Eggstein G, Liebner S, Hamm S, Duffner F, Grote E-H, Risau W, Engelhardt B (2003) Localization of claudin-3 in tight junctions of the blood–brain barrier is selectively lost during experimental autoimmune encephalomyelitis and human glioblastoma multiforme. Acta Neuropathol 105:586–592

Xiang S, Pan W, Kastin AJ (2005) Strategies to create a regenerating environment for the injured spinal cord. Curr Pharm Des 11:1267–1277